Approximation of Uplink Inter-Cell Interference in FDMA Small Cell Networks

Ming Ding, *National ICT Australia (NICTA), Australia* {Ming.Ding@nicta.com.au}
David López Pérez, *Bell Labs Alcatel-Lucent, Ireland* {dr.david.lopez@ieee.org}
Guoqiang Mao, *The University of Technology Sydney and NICTA, Australia* {Guoqiang.Mao@uts.edu.au}
Zihuai Lin, *The University of Sydney, Australia* {zihuai.lin@sydney.edu.au}

arXiv:1505.01924v3 [cs.NI] 26 Sep 2017

***Abstract*—In this paper, for the first time, we analytically prove that the uplink (UL) inter-cell interference in frequency division multiple access (FDMA) small cell networks (SCNs) can be well approximated by a lognormal distribution under a certain condition. The lognormal approximation is vital because it allows tractable network performance analysis with closed-form expressions. The derived condition, under which the lognormal approximation applies, does not pose particular requirements on the shapes/sizes of user equipment (UE) distribution areas as in previous works. Instead, our results show that if a path loss related random variable (RV) associated with the UE distribution area, has a low ratio of the 3rd absolute moment to the variance, the lognormal approximation will hold. Analytical and simulation results show that the derived condition can be readily satisfied in future dense/ultra-dense SCNs, indicating that our conclusions are very useful for network performance analysis of the 5th generation (5G) systems with more general cell deployment beyond the widely used Poisson deployment.** [1]

I. Introduction

Small cell networks (SCNs) have been identified as one of the key enabling technologies in the 5th generation (5G) networks [1]. In order to gain a deep theoretical understanding of the implications that SCNs bring about, new and more powerful network performance analysis techniques are being developed. In this context, new performance analysis tools can be broadly classified into two large groups, i.e., macro-scopic analysis and micro-scopic analysis [2-8].

The macro-scopic analysis assumes that both user equipments (UEs) and small cell base stations (BSs) are randomly placed in the network, often following homogeneous Poisson distributions [2,3]. The micro-scopic analysis is usually conducted assuming that UEs are randomly dropped and the BSs are deterministically deployed, i.e., the BS positions in the considered cellular network are known. Generally speaking, the macro-scopic analysis investigates network performance on a high level [2,3], while the micro-scopic analysis gives more detailed results for specific networks [4-8]. Note that both analyses are related to each other. The average performance of micro-scopic analyses conducted over a large number of realizations of BS deployments should be equal to that of the macro-scopic analysis, provided that the examined realizations of the deterministic BS deployments follow the BS distribution assumed in the corresponding macro-scopic analysis.

In this paper, we focus on the micro-scopic analysis, and in particular, we consider an uplink (UL) frequency division multiple access (FDMA) SCN. Note that the analysis of a UL FDMA system is more involved than its downlink counterpart due to the power control mechanisms used at UEs. For the UL micro-scopic analysis, existing works either use

- Approach 1, which provides closed-form but complicated analytical results for a network with *a small number of interfering cells, each cell with a regularly-shaped UE distribution area*, e.g., a disk or a hexagon [4];
- Approach 2, which makes a empirical conjecture on the UL interference distribution and on that basis derives analytical results for a network with *multiple interfering cells placed on a regularly-shaped lattice*, e.g., a hexagonal lattice [5], [6];
- Approach 3, which conducts system-level simulations to directly obtain empirical results for a complex network with *practical deployment of multiple cells placed on irregular locations* [1], [7], [8].

Obviously, Approach 1 and Approach 3 lack generality and analytical rigorousness, respectively. Regarding Approach 2, it has been a number of years since an important conjecture was proposed and extensively used in performance analysis, which stated that the UL inter-cell interference with disk-shaped UE distribution areas could be well approximated by a lognormal distribution in code division multiple access (CDMA) SCNs [5] and in FDMA SCNs [6]. This conjecture is vital since it allows tractable network performance analysis with closed-form expressions. However, there are two intriguing questions regarding this conjecture: *(i) Will the approximation still hold for non-disk-shaped UE distribution areas? (ii) Will it depend on the sizes of the UE distribution areas?* In this paper, we aim to answer those two questions, and thus making significant contributions to constructing a formal tool for the UL micro-scopic analysis of network performance.

Compared with the previous works [5,6] of the micro-scopic network performance analysis based on empirical studies, the contributions of this paper are as follows:

1) Our work, for the first time, analytically proves the conjecture in [6], i.e., the UL inter-cell interference in FDMA SCNs can be well approximated by a lognormal

[1]1536-1276 © 2015 IEEE. Personal use is permitted, but republication/redistribution requires IEEE permission. Please find the final version in IEEE from the link: http://ieeexplore.ieee.org/document/7417160/. Digital Object Identifier: 10.1109/GLOCOM.2015.7417160

distribution under a certain condition.

2) The derived condition, under which the lognormal approximation applies, does not rely on particular shapes/sizes of UE distribution areas and can be readily satisfied in future dense/ultra-dense SCNs, indicating that conclusions derived using this framework are very general and useful for network performance analysis.
3) Based on our work, we propose a new approach to fill an important theoretical gap in the existing microscopic analysis, which either assumes very simple BS deployments or relies on empirical results. Specifically, we directly investigate a complex network with *practical deployment of multiple cells placed on irregular locations*. In order to do that we provide a theoretical framework based on the lognormal approximation of the UL interference distribution, supported by rigorous theoretical analysis, as well as the conditions under which the approximation should be valid.

II. Network Scenario and System Model

In this paper, we consider UL transmissions and assume that in one frequency resource block (RB) at a time slot, only *one* UE is scheduled by each small cell BS to perform an UL transmission, which is a reasonable assumption in line with the 4th generation (4G) networks, i.e., the UL single-carrier FDMA (SC-FDMA) system and the UL orthogonal FDMA (OFDMA) system in the 3rd Generation Partnership Project (3GPP) Long Term Evolution (LTE) networks [9] and in the Worldwide Interoperability for Microwave Access (WiMAX) networks [10], respectively.

Regarding the network scenario, we consider a SCN with multiple small cells operating on the same carrier frequency as shown in Fig. 1. In Fig. 1, a total of B small cells exist in the network, including one small cell of interest denoted by C_1 and $B-1$ interfering small cells denoted by $C_b, b \in \{2,\ldots,B\}$. We consider a particular frequency RB, and denote by K_b the active UE associated with small cell C_b using that frequency RB. Moreover, we denote by R_b *the UE distribution area* of small cell C_b, in which its associated UEs are distributed.

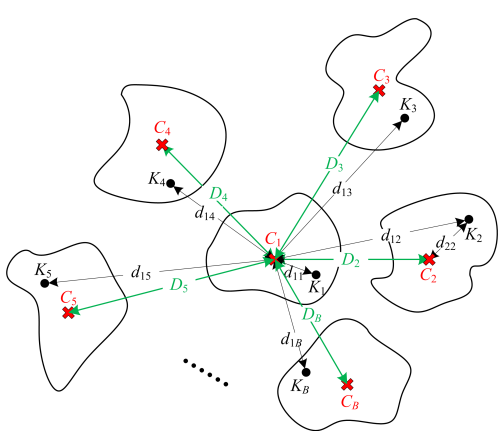

Fig. 1. A schematic model of the considered SCN.

The distance (in km) from the BS of C_b to the BS of C_1, $b \in \{1,\ldots,B\}$ and the distance from UE K_b to the BS of C_m, $b,m \in \{1,\ldots,B\}$ are denoted by D_b and d_{bm}, respectively. In this paper, we consider a deterministic deployment of BSs, and thus $\{D_b\}$ is assumed to be known. However, the position of UE K_b is assumed to be randomly and uniformly distributed in R_b. Hence, d_{bm} is a random variable (RV), the distribution of which cannot be readily expressed in analytical form due to the arbitrary shape of R_b.

Based on the definition of d_{bm}, *the path loss* (in dB) from UE K_b to the BS of C_m is modeled as

$$L_{bm} = A + \alpha \log_{10} d_{bm}, \tag{1}$$

where A and α are the path loss at the reference distance $d_{bm}=1$ and the path loss exponent, respectively. Note that L_{bm} is a RV due to the randomness of d_{bm}. In practice, A and α are constants obtainable from field tests [12].

The shadow fading (in dB) from UE K_b to the BS of C_m is denoted by S_{bm} $(b,m \in \{1,\ldots,B\})$, and it is usually modeled as a zero-mean Gaussian RV because the linear value of S_{bm} is commonly assumed to follow a lognormal distribution [12]. Hence, in this paper, we model S_{bm} as an independently identical distributed (i.i.d.) zero-mean Gaussian RV with variance σ^2_{Shad}, expressed as $S_{bm} \sim \mathcal{N}\left(0, \sigma^2_{\text{Shad}}\right)$[2].

The multi-path fading channel vector from UE K_b to the BS of C_m is denoted by $\mathbf{h}_{bm} \in \mathbb{C}^{N\times 1}$, where we assume that each UE and each BS are equipped with 1 and N omni-directional antennas, respectively. All channel coefficients are assumed to experience uncorrelated flat Rayleigh fading, and they are modeled as i.i.d. zero-mean circularly symmetric complex Gaussian (ZMCSCG) RVs with unit variance.

The normalized maximal ratio combining (MRC) reception filter denoted by $\mathbf{f}_m = \frac{\mathbf{h}^{\text{H}}_{mm}}{\|\mathbf{h}_{mm}\|}$ is considered at the BS of C_m, where $\mathbf{h}^{\text{H}}_{mm}$ is the Hermitian transpose of $\mathbf{h}_{mm}$. According to [11], the effective channel gain associated with the link from UE K_b to the BS of C_m $(b,m \in \{1,\ldots,B\}, b \neq m)$, defined as $|\mathbf{f}_m \mathbf{h}_{bm}|^2$ and denoted by H_{bm}, follows an i.i.d. exponential distribution $\exp(1)$ with the mean equal to 1.

The transmit power of UE K_b is denoted by P_b. In practice, P_b is usually subject to a semi-static power control (PC) mechanism, e.g., the fractional pathloss compensation (FPC) scheme [12]. Specifically, based on this FPC scheme, P_b in dBm is modeled as[3]

$$P_b = P_0 + \eta\left(L_{bb} + S_{bb}\right), \tag{2}$$

[2]A more practical assumption would be the correlated shadow fading [13], which constructs S_{bm} and S_{jm} $(b,j,m \in \{1,\ldots,B\}, b \neq j)$ as correlated RVs, and the correlation coefficient should decrease with the increase of the distance from UE K_b to UE K_j. Such assumption of the correlated shadow fading will greatly complicate the analysis since it is difficult to characterize the distribution of the inter-UE distance. For the sake of tractability, in this paper, we assume i.i.d. shadow fading for the UE-to-BS links.

[3]In practice, P_b is also constrained by the maximum value of the UL power and affected by the per-UE signal-to-interference-plus-noise ratio (SINR) target. The power constraint is a minor issue for UEs in SCNs since they are generally not power-limited due to the close proximity of the UEs and the associated SCN BSs [12]. The per-UE SINR target, on the other hand, will greatly complicate the analysis since it is difficult to model the distribution of the target SINRs. For the sake of tractability, in this paper, we model P_b as (2), which is widely adopted in the literature [3,6-8,11].

Table I
DEFINITION OF RVS.

RV	Description	Distribution
d_{bm}	The distance from K_b to C_m	related to R_b
L_{bm}	The path loss from K_b to C_m	related to R_b
S_{bm}	The shadow fading from K_b to C_m	i.i.d. $\mathcal{N}\left(0, \sigma_{\text{Shad}}^2\right)$
H_{bm}	The channel gain from K_b to C_m	i.i.d. $\exp(1)$
P_b	The UL transmission power of K_b	related to R_b

where P_0 is the power basis in dBm on the considered frequency RB, $\eta \in (0, 1]$ is the FPC factor, L_{bb} has been defined in (1), and $S_{bb} \sim \mathcal{N}\left(0, \sigma_{\text{Shad}}^2\right)$.

For clarity, the defined RVs in our system model are summarized in Table I.

III. ANALYSIS OF UL INTERFERENCE

Based on the definition of RVs listed in Table I, *the UL received interference power* (in dBm) from UE K_b to the BS of C_1 can be written as

$$\begin{aligned} I_b &\overset{(a)}{=} P_b - L_{b1} - S_{b1} + 10\log_{10} H_{b1} \\ &= P_0 + (\eta L_{bb} - L_{b1}) + (\eta S_{bb} - S_{b1}) + 10\log_{10} H_{b1} \\ &\overset{\triangle}{=} P_0 + L + S + 10\log_{10} H_{b1}, \end{aligned} \tag{3}$$

where (2) is plugged into step (a) of (3). Besides, L and S are defined as $L \overset{\triangle}{=} (\eta L_{bb} - L_{b1})$ and $S \overset{\triangle}{=} (\eta S_{bb} - S_{b1})$, respectively. In particular, since S_{bb} and S_{b1} ($b \in \{2, \ldots, B\}$) are i.i.d. zero-mean Gaussian RVs, it is easy to show that S is also a Gaussian RV with a distribution $\mathcal{N}\left(\mu_S, \sigma_S^2\right)$, where

$$\begin{cases} \mu_S = 0 \\ \sigma_S^2 = \left(1 + \eta^2\right)\sigma_{\text{Shad}}^2 \end{cases}. \tag{4}$$

From the definition of I_b in (3), *the aggregated interference power* (in mW) from all interfering UEs to the BS of C_1 is

$$I^{\text{mW}} = \sum_{b=2}^{B} 10^{\frac{1}{10} I_b}. \tag{5}$$

In the following, we analyze the distribution of I^{mW} in three steps. First, we investigate the distribution of $(S + 10\log_{10} H_{b1})$ shown in (3). Second, we approximate the distribution of I_b as a Gaussian distribution. Third, we show that the distribution of I^{mW} can be further approximated as a lognormal distribution.

A. The Distribution of $(S + 10\log_{10} H_{b1})$ in (3)

According to [14], the product of a lognormal RV and an exponential RV can be well approximated by another lognormal RV. Therefore, in our case, the sum $(S + 10\log_{10} H_{b1})$ can be well approximated by a Gaussian RV G, because $10^{\frac{1}{10}S}$ is a lognormal RV and $H_{b1} \sim \exp(1)$. The mean and variance of G can be respectively computed as [14]

$$\begin{cases} \mu_G = \mu_S + \mu_{\text{offset}} \\ \sigma_G^2 = \sigma_S^2 + \sigma_{\text{offset}}^2 \end{cases}. \tag{6}$$

In [14], μ_{offset} and σ_{offset} are suggested to be -2.5 and 5.57, respectively. Note that the approximation is very accurate when $\sigma_S^2 > 36$ [14]. Such requirement is readily satisfied in practical SCNs, e.g., it is recommended in [12] that $\sigma_{\text{Shad}}^2 = 100$ and hence $\sigma_S^2 > 100 > 36$ because of (4).

B. The Distribution of I_b in (3)

In the following, we will prove that under a certain condition, I_b can be well approximated by a Gaussian RV. First, based on the approximation discussed in Subsection III-A, we reform (3) into

$$I_b \approx P_0 + L + G. \tag{7}$$

Note that the probability density function (PDF) and cumulative density function (CDF) of L are generally not tractable because L is a RV with respect to d_{bb} and d_{b1}, which jointly depend on the arbitrary shape of R_b.

Next, we analyze the distribution of I_b by investigating the condition under which the sum of a Gaussian RV and an arbitrary RV, i.e., $(L + G)$, can be well approximated by another Gaussian RV. To that end, we denote by μ_L and σ_L^2 the mean and variance of L, respectively, define a zero-mean RV as $\tilde{L} = L - \mu_L$, and further define another zero-mean RV as $\tilde{G} = G - \mu_G$. As a result, (7) can be re-written as

$$I_b \approx \tilde{L} + \tilde{G} + (P_0 + \mu_L + \mu_G). \tag{8}$$

1) The distribution of $\left(\tilde{L} + \tilde{G}\right)$ in (8):

Obviously, if $\left(\tilde{L} + \tilde{G}\right)$ in (8) can be well approximated by a Gaussian RV, then I_b can also be well approximated by the same Gaussian RV with an offset $(P_0 + \mu_L + \mu_G)$. In order to prove that $\left(\tilde{L} + \tilde{G}\right)$ indeed can be well approximated by a Gaussian RV, we introduce the Berry–Esseen theorem in Theorem 1.

Theorem 1. *[Theorem 1, 15] The Berry–Esseen theorem: Let $X_1, X_2, \ldots, X_M$ be M independent RVs with $\mathbb{E}\{X_i\} = 0$, $\mathbb{E}\left\{X_i^2\right\} = \sigma_i^2 > 0$, and $\mathbb{E}\left\{|X_i|^3\right\} < \infty$, $i \in \{1, 2, \ldots, M\}$. Also, let $X = \frac{\sum_{i=1}^{M} X_i}{\sqrt{\sum_{i=1}^{M} \sigma_i^2}}$. Denote by $F_X(x)$ and $\Phi(x)$ the CDF of X and the CDF of the standard normal distribution. Then, we have*

$$\sup_{x \in \mathbb{R}} |F_X(x) - \Phi(x)| \leq C_0 \psi_0, \tag{9}$$

where $\psi_0 = \frac{\sum_{i=1}^{M} \mathbb{E}\left\{|X_i|^3\right\}}{\left(\sqrt{\sum_{i=1}^{M} \sigma_i^2}\right)^3}$ and $C_0 = 0.56$.

In Theorem 1, $C_0\psi_0$ is the upper bound of the maximum gap between $F_X(x)$ and $\Phi(x)$. Therefore, Theorem 1 shows *how good* the sum of M independent RVs can be approximated by a Gaussian RV. As long as $C_0\psi_0$ is reasonably small, we can say that the approximation is good. Based on Theorem 1, we propose Lemma 2 to address the question: Under what condition can $\left(\tilde{L} + \tilde{G}\right)$ in (8) be well approximated by a Gaussian RV?

Lemma 2. *Considering the zero-mean RV* $\left(\tilde{L}+\tilde{G}\right)$ *given by (8), we define a normalized RV as* $Y=\frac{\tilde{L}+\tilde{G}}{\sqrt{\sigma_L^2+\sigma_G^2}}$. *Denote by* $F_Y(y)$ *and* $\Phi(y)$ *the CDF of* Y *and the CDF of the standard normal distribution. Then, we have*

$$\sup_{y\in\mathbb{R}}\left|F_Y(y)-\Phi(y)\right|\leq\tau, \tag{10}$$

where $\tau=\frac{C_0\mathbb{E}\left\{\left|\tilde{L}\right|^3\right\}}{\left(\sqrt{\sigma_L^2+\sigma_G^2}\right)^3}$ *and* $C_0=0.56$.

Proof: In order to make use of Theorem 1 to prove Lemma 2, we construct $M-1$ zero-mean Gaussian RVs by breaking the zero-mean Gaussian RV $\tilde{G}$ into the sum of $M-1$ i.i.d. zero-mean Gaussian RVs $\{G_i\}, i\in\{1,2,\ldots,M-1\}$, i.e., $\tilde{G}=\sum_{i=1}^{M-1}G_i$. The variance of each G_i is $\sigma_{G_i}^2=\frac{\sigma_G^2}{M-1}$. Hence, the constructed $M-1$ zero-mean Gaussian RVs $\{G_i\}$ and the RV $\tilde{L}$ form the set of M i.i.d. RVs required to invoke Theorem 1. Denote the normalized sum of the M RVs as $Y=\frac{\tilde{L}+\sum_{i=1}^{M-1}G_i}{\sqrt{\sigma_L^2+\sum_{i=1}^{M-1}\sigma_{G_i}^2}}$. Then, we can evaluate the upper bound of the maximum gap between $F_Y(y)$ and $\Phi(y)$ by checking the metric $C_0\psi_0$ using Theorem 1.

According to Theorem 1, the metric $C_0\psi_0$ for Y becomes

$$\begin{aligned}C_0\psi_0&\overset{(a)}{=}C_0\times\frac{\mathbb{E}\left\{\left|\tilde{L}\right|^3\right\}+\sum_{i=1}^{M-1}\mathbb{E}\left\{\left|G_i\right|^3\right\}}{\left(\sqrt{\sigma_L^2+\sum_{i=1}^{M-1}\sigma_{G_i}^2}\right)^3}\\&=C_0\times\frac{\mathbb{E}\left\{\left|\tilde{L}\right|^3\right\}+\frac{(M-1)\left(\sqrt{2}\right)^3\Gamma(2)}{\sqrt{\pi}}\left(\sqrt{\frac{\sigma_G^2}{M-1}}\right)^3}{\left(\sqrt{\sigma_L^2+\sigma_G^2}\right)^3},\end{aligned} \tag{11}$$

where $\mathbb{E}\left\{\left|G_i\right|^3\right\}=\frac{\left(\sqrt{2}\right)^3\Gamma(2)}{\sqrt{\pi}}\left(\sqrt{\frac{\sigma_G^2}{M-1}}\right)^3$ [16] has been plugged into step (a) of (11). Since the value of M is arbitrary in Theorem 1, we let M approach infinity, and thus the first term of the numerator of ψ_0 in (11), i.e., $\frac{(M-1)\left(\sqrt{2}\right)^3\Gamma(2)}{\sqrt{\pi}}\left(\sqrt{\frac{\sigma_G^2}{M-1}}\right)^3$, will diminish to zero and as a result $C_0\psi_0$ converges to τ given by

$$\tau=\frac{C_0\mathbb{E}\left\{\left|\tilde{L}\right|^3\right\}}{\left(\sqrt{\sigma_L^2+\sigma_G^2}\right)^3}. \tag{12}$$

Our proof is thus completed. ■

An important note on the proof of Lemma 2 is that the decomposition of $\tilde{G}$ into the sum of $M-1$ i.i.d. zero-mean Gaussian RVs $\{G_i\}$ allows the diminishing of $\sum_{i=1}^{M-1}\mathbb{E}\left\{\left|G_i\right|^3\right\}$, which quickly reduces $C_0\psi_0$ in (11) to τ, thus making it much easier for the Gaussian approximation to be valid. According to Theorem 1, if τ in (12) takes a reasonably small value, then $\left(\tilde{L}+\tilde{G}\right)$ can be well approximated by a Gaussian RV.

From Lemma 2, we can see that τ decreases with the decrease of $\mathbb{E}\left\{\left|\tilde{L}\right|^3\right\}$ and with the increase of σ_G^2 and σ_L^2. Therefore, if the $\frac{\mathbb{E}\left\{\left|\tilde{L}\right|^3\right\}}{\sigma_L^2}$ associated with UE distribution area R_b is low, then τ tends to be a small value, and hence the approximation holds. Intuitively speaking, if $\frac{\mathbb{E}\left\{\left|\tilde{L}\right|^3\right\}}{\sigma_L^2}$ is low, then the interfering UEs will be basically concentrated in a small area of R_b. As a result, the geometrical randomness of the interfering UEs is reduced, and hence the dB-scale shadow fading, usually modeled as Gaussian distributions, will dominate the dB-scale UL interference distribution. Also, a larger σ_G^2 allows a better approximation due to the more dominance of the Gaussian distribution of the dB-scale shadow fading. It is important to note that although the PDF and CDF of L and $\tilde{L}$ are difficult to obtain, if not impossible, the values of σ_L^2, $\mathbb{E}\left\{\left|\tilde{L}\right|^3\right\}$ can be easily computed using numerical integration over the UE distribution area R_b. We will briefly discuss the calculation of τ in the next subsection.

To sum up, according to Lemma 2, if τ is reasonably small for the considered SCN, e.g., around 0.01 (an error about 1 percentile), $\left(\tilde{L}+\tilde{G}\right)$ can be well approximated by a zero-mean Gaussian RV. Then, I_b in (8) can be well approximated by a Gaussian RV Q_b, the mean and the variance of which can be computed by

$$\begin{cases}\mu_{Q_b}=P_0+\mu_L+\mu_G\\ \sigma_{Q_b}^2=\sigma_L^2+\sigma_G^2\end{cases}. \tag{13}$$

2) The calculation of τ*:*

Considering the definition of L, $\tilde{L}$ respectively in (3) and (8), we can directly evaluate τ using (12) based on the results of μ_L, σ_L^2 and $\mathbb{E}\left\{\left|\tilde{L}\right|^3\right\}$ computed by

$$\begin{aligned}\mu_L&=\int_{R_b}L dZ\\&=\int_{R_b}\left(\eta L_{bb}-L_{b1}\right)dZ\\&=\int_{R_b}\left((\eta-1)A+\alpha\log_{10}\frac{d_{bb}^{\eta}}{d_{b1}}\right)dZ.\end{aligned} \tag{14}$$

$$\begin{aligned}\sigma_L^2&=\int_{R_b}\left(L-\mu_L\right)^2dZ\\&=\int_{R_b}\left((\eta-1)A+\alpha\log_{10}\frac{d_{bb}^{\eta}}{d_{b1}}-\mu_L\right)^2dZ.\end{aligned} \tag{15}$$

$$\begin{aligned}\mathbb{E}\left\{\left|\tilde{L}\right|^3\right\}&=\int_{R_b}\left|L-\mu_L\right|^3dZ\\&=\int_{R_b}\left|(\eta-1)A+\alpha\log_{10}\frac{d_{bb}^{\eta}}{d_{b1}}-\mu_L\right|^3dZ.\end{aligned} \tag{16}$$

C. The Distribution of I^{mW} *in (5)*

According to [17], the sum of multiple independent lognormal RVs can be well approximated by a lognormal RV. Considering the expression of I^{mW} in (5), if each $I_b, b\in\{2,\ldots,B\}$ can be approximated by the Gaussian RV Q_b, we can conclude that I^{mW} can be well approximated by a lognormal RV, denoted by $\hat{I}^{\mathrm{mW}}=10^{\frac{1}{10}Q}$. The RV Q is a Gaussian RV and its mean and the variance are denoted by μ_Q and σ_Q^2, respectively. According to [17], μ_Q and σ_Q^2 are obtained by solving the following equation set,

$$\begin{cases} \hat{\Psi}_Q(s_1) = \prod_{b=2}^{B} \hat{\Psi}_{Q_b}(s_1) \triangleq C_1 \\ \hat{\Psi}_Q(s_2) = \prod_{b=2}^{B} \hat{\Psi}_{Q_b}(s_2) \triangleq C_2 \end{cases}, \quad (17)$$

where $\hat{\Psi}_X(s)$ is the approximated moment generating function (MGF) evaluated at s for a lognormal RV defined as $10^{\frac{1}{10}X}$. Such approximated MGF is formulated as

$$\hat{\Psi}_X(s) = \sum_{m=1}^{M_0} \frac{w_m}{\sqrt{\pi}} \exp\left(-s \exp\left(\frac{\sqrt{2\sigma_X^2} a_m + \mu_X}{\zeta}\right)\right), \quad (18)$$

where $\zeta = \frac{10}{\ln 10}$, M_0 is the order of the Gauss-Hermite numerical integration, the weights w_m and abscissas a_m for M_0 up to 20 are tabulated in Table 25.10 in [18]. Usually, M_0 is larger than 8 to achieve a good approximation [17].

In (17), s_1 and s_2 are two design parameters for generating two equations that can determine the appropriate values of μ_Q and σ_Q^2. Generally speaking, when s_1 and s_2 take smaller (larger) values, the mismatch in the head (tail) portion between the actual CDF and the approximated one can be reduced [17]. The basic idea of (17) is to let the two concerned RVs, i.e., I^{mW} and $\hat{I}^{\text{mW}}$, statistically match with each other in the sense of having two equal points on their MGFs. The solution of (17) can be readily found by standard mathematical software programs such as MATLAB.

Based on this lognormal approximation, the approximated PDF and CDF of I^{mW} can be respectively expressed as [16]

$$f_{I^{\text{mW}}}(v) \approx \frac{\zeta}{v\sqrt{2\pi\sigma_Q^2}} \exp\left\{-\frac{(\zeta \ln v - \mu_Q)^2}{2\sigma_Q^2}\right\}, \quad (19)$$

and

$$F_{I^{\text{mW}}}(v) \approx \frac{1}{2} + \frac{1}{2}\text{erf}\left(\frac{\zeta \ln v - \mu_Q}{\sqrt{2\sigma_Q^2}}\right), \quad (20)$$

where $\text{erf}(\cdot)$ is the error function.

D. Summary of the Proposed Analysis of UL Interference

To sum up, we highlight the steps in our proposed analysis of UL interference in the following. First, we use (14), (15) and (16) to calculate μ_L, σ_L^2 and $\mathbb{E}\left\{\left|\tilde{L}\right|^3\right\}$ for each $R_b, b \in \{2, \ldots, B\}$. Then, based on the calculated results, we check whether τ given by Lemma 2 is reasonably small. If it is the case, we can approximate I_b as a Gaussian RV Q_b according to the discussion in Subsection III-B. Finally, we approximate the RV I^{mW} in (5) as a lognormal RV $\hat{I}^{\text{mW}} = 10^{\frac{1}{10}Q}$, with the distribution parameters μ_Q and σ_Q^2 obtained from solving the equation set (17). The chain of approximation to obtain $\hat{I}^{\text{mW}}$ is summarized in Table II shown on the top of next page.

IV. Simulation and Discussion

In order to validate the results from the proposed microscopic analysis of UL interference, we conduct simulations considering two scenarios, with a single interfering cell and with multiple interfering cells, respectively. According to the 3GPP standards [12], the system parameters in our simulations are set to: $A = 103.8$, $\alpha = 20.9$, $P_0 = -76$ dBm, $\eta = 0.8$, and $\sigma_S^2 = 100$. Besides, the minimum BS-to-UE distance is assumed to be 0.005 km [12]. Regarding the equation set (17) to determine μ_Q and σ_Q^2, we choose the parameters as $s_1 = 1$, $s_2 = 0.1$ and $M_0 = 12$ as recommended in [17].

A. The Scenario with a Single Interfering Cell

In this scenario, we consider $B = 2$, as shown in Fig. 2. The x-markers indicate BS locations, where the BS location of C_1 has been explicitly pointed out. The dash-dot line indicate a reference disk to illustrate the reference size of small cell C_2. The radius of such reference circle is denoted by r, and the distance between the BS of C_1 and the BS of C_2, i.e., D_2, is assumed to be $1.5r$. In our simulations, the values of r (in km) are set to 0.01, 0.02 and 0.04, respectively. In this scenario, the interfering UE K_2 is randomly and uniformly distributed in an irregularly shaped UE distribution area R_2, as illustrated by the area outlined using solid line in Fig. 2. The shape of R_2 is the intersection of a square, a circle and an ellipse, which has a complicated generation function. Examples of the possible positions of K_2 within R_2 are shown as dots.

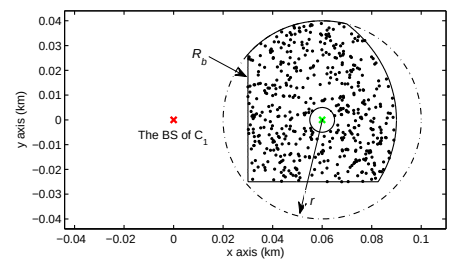

Fig. 2. Illustration of R_2 (irregular shape, $r = 0.04$).

Table III
Results of the proposed analysis ($B = 2$).

The value of r	τ	μ_{Q_2}	$\sigma_{Q_2}^2$
$r = 0.01$	0.0082	-97.10	205.25
$r = 0.02$	0.0122	-99.69	207.73
$r = 0.04$	0.0184	-101.54	211.44

Despite of the complicated shape of R_2, our proposed lognormal approximation of the UL interference still works. Specifically, from (14), (15), (16) and Lemma 2, we can calculate μ_L, σ_L^2, $\mathbb{E}\left\{\left|\tilde{L}\right|^3\right\}$ and τ, respectively. The results of τ are tabulated for various values of r in Table III. From Table III, we can observe that, when $r = 0.01$ or 0.02, the values of τ are around 0.01. Consequently, it indicates a good approximation of I_2 as a Gaussian RV. Note that $r = 0.01$ and $r = 0.02$ correspond to the typical network configurations for future dense/ultra-dense SCNs [1], which shows that the derived condition in Lemma 2 can be readily used to study future dense/ultra-dense SCNs.

To confirm the accuracy of the proposed approximation summarized in Table II, we plot the approximated analytical

Table II
THE CHAIN OF APPROXIMATION TO OBTAIN $\hat{I}^{\text{MW}}$.

Original RV	Approximated RV	Approximated distribution	Distribution parameters
$S + 10\log_{10} H_{b1}$ in (3)	G	Gaussian	See (6)
$I_b \approx P_0 + L + G$ in (7)	Q_b	Gaussian	See (13)
$I^{\text{mW}} = \sum_{b=2}^{B} 10^{\frac{1}{10} I_b}$ in (5)	$\hat{I}^{\text{mW}}$	Lognormal	The solution of (17)

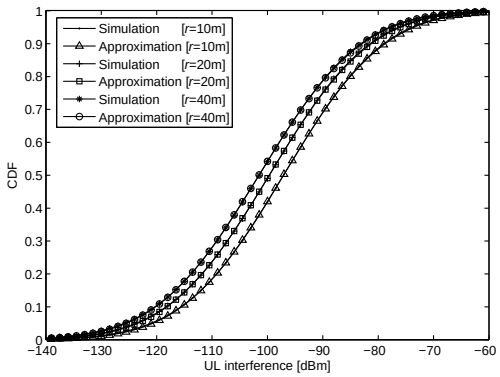

Fig. 3. The simulation and approximation of I_2 (irregular shape of R_2).

results and the simulation results of I_2 for the considered R_2 in Fig. 3. Also, the numerical results of μ_{Q_2} and $\sigma^2_{Q_2}$ are shown in Table III. As can be seen from Fig. 3, the proposed Gaussian approximation of I_2 is indeed very tight for the considered R_2 with such an irregular shape. Note that the approximation appears to be very good even for $r = 0.04$ (despite a relatively large value of τ at around 0.02), which implies that the derived condition in Lemma 2 might be too strict and the proposed approximation might be extended to more general conditions. Hence, it is our future work to find a way to relax the sufficient condition proposed in Lemma 2 to allow for a wider application of the proposed analysis.

B. The Scenario with Multiple Interfering Cells

The lognormal approximation of the UL interference for a network with *multiple interfering cells placed on a hexagonal lattice* has been validated in [6]. As a significant leap from the hexagonal network, in this subsection, we apply the proposed framework on a more complex network with *practical deployment of multiple cells* and provide the approximation of the UL interference distribution.

Here, we consider a 3GPP-compliant scenario [12], as shown in Fig. 4. In Fig. 4, B is set to 84 and all small cell BSs are represented by x-markers. Particularly, the BS of C_1 has been explicitly pointed out. The reference UE distribution area for each small cell is a disk with a radius of r [12]. In our simulations, the values of r (in km) are set to 0.01, 0.02 and 0.04, respectively. The reference disk-shaped areas can be easily seen in Fig. 4 from any isolated small cell. However, due to the irregular positions of the cells, the actual UE distribution areas of the considered cells are of irregular shapes due to cell overlapping. The irregularly shaped UE distribution areas are outlined in Fig. 4 by solid lines. Interfering UEs are randomly and uniformly distributed in those areas. An important note is that the considered network scenario is different from that

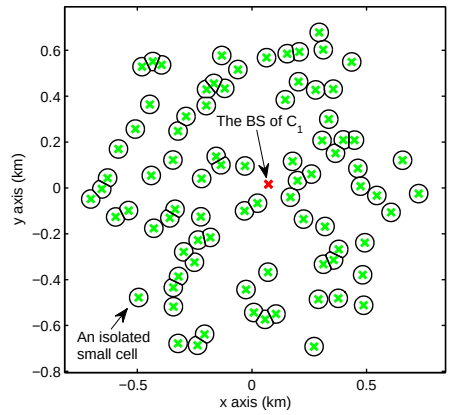

Fig. 4. Illustration of a practical deployment of multiple cells ($r = 0.04$).

adopted in [2,3], where UE distribution areas are defined as Voronoi cells generated by the Poisson distributed BSs and those Voronoi cells cover the whole network area. In practice, small cells are mainly used for capacity boosting in specific populated areas, rather than provision of an umbrella coverage for all UEs. Therefore, the 3GPP standards recommend the hotspot SCN scenario depicted in Fig. 4 for UE distribution in the performance evaluation of practical SCNs. Nevertheless, the proposed micro-scopic analysis of UL interference can still be applied on a particular Voronoi tessellation, since the derived condition in Lemma 2 does not rely on particular shapes/sizes of UE distribution areas.

To the best knowledge of the authors, the micro-scopic analysis of UL interference for such complex network as shown in Fig. 4 has never been attempted before in the literature. Now, we investigate the considered network with the proposed approach of performance analysis. First, we use (14), (15) and (16) to calculate μ_L, σ^2_L and $\mathbb{E}\left\{\left|\tilde{L}\right|^3\right\}$ for *each* $R_b, b \in \{2, \ldots, 84\}$ displayed in Fig. 4. Then, based on the calculated results, we check the value of τ for *each* R_b using Lemma 2. The maximum values of the 83 R_b-specific τ's for various r values are presented in Table IV. It is shown in the table that when $r = 0.01$ and $r = 0.02$ the maximum τ is below or around 0.01, and thus each I_b can be approximated by a Gaussian RV Q_b according to the discussion in Subsection III-B. Again, note that $r = 0.01$ and $r = 0.02$ correspond to the typical network configurations for future dense/ultra-dense SCNs [1], which indicates the usefulness of the proposed approach of the micro-scopic analysis in future 5G SCNs. Finally, we approximate the RV I^{mW} in (5) as a lognormal RV $\hat{I}^{\text{mW}} = 10^{\frac{1}{10}Q}$, with the distribution parameters μ_Q and σ^2_Q obtained from solving the equation set (17). The

numerical results of μ_Q and σ_Q^2 are provided in Table IV.

Table IV
RESULTS OF THE PROPOSED ANALYSIS ($B = 84$).

The value of r	Maximum τ	μ_Q	σ_Q^2
$r = 0.01$	0.0066	-75.09	17.77
$r = 0.02$	0.0125	-77.21	18.30
$r = 0.04$	0.0176	-78.76	18.55

To validate the accuracy of our results on the UL interference, we plot the approximated analytical results and the simulation results of I^{mW} in dBm for the considered network in Fig. 5. As can be seen from Fig. 5, the resulting lognormal approximation of I^{mW} is reasonably good for practical use. Note that the approximation shown in Fig. 5 is not as tight as that exhibited in Fig. 3. The noticeable approximation errors in Fig. 5 are mostly caused by the inaccuracy of approximating the sum of multiple lognormal RVs as a single lognormal RV in [17]. Note that the parameters of $s_1 = 1$ and $s_2 = 0.1$ recommended by [17] allow for an overall match between the actual CDF and the approximated lognormal CDF, though the approximation in the head portion and the tail portion of the CDF are compromised to some extent. Hence, a straightforward way to improve the approximation of UL interference shown in Fig. 5 is to approximate the CDF of I^{mW} as a piece-wise lognormal CDFs, because smaller (larger) s_1 and s_2 are helpful to increase the quality of approximation in the head (tail) portion of the considered CDF [17]. Regarding the individual approximation of I_b as a Gaussian RV Q_b, we find that it is tight for every considered R_b. Due to space limitation, we omit the investigation on the Gaussian approximation for each I_b, which is quite similar to the discussion in Subsection IV-A.

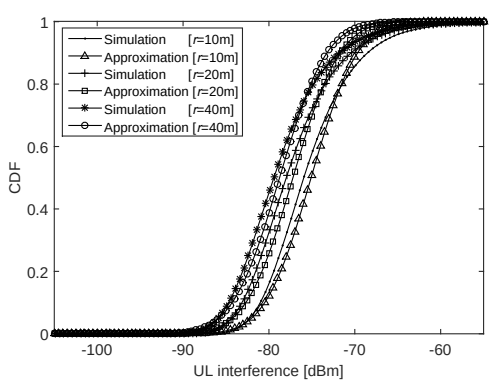

Fig. 5. The simulation and approximation of I^{mW} in dBm.

A final note on the proposed network performance analysis is that our approach is very powerful to obtain the analytical results in an efficient manner. The computational complexity is mainly attributable to the numerical integration to obtain the values of μ_L, σ_L^2 and $\mathbb{E}\left\{\left|\tilde{L}\right|^3\right\}$ for the 83 interfering cells. In contrast, the simulation involves a tremendously high complexity. Specifically, in our simulations, around *one billion* of realizations of I_b have been conducted for the 83 interfering cells in order to go through the randomness of all the RVs listed in Table I. This shows that the proposed micro-scopic analysis of network performance is elegant and computationally efficient, which makes it ideal to study future 5G systems with general and dense small cell deployments.

V. CONCLUSION

The conjecture of approximating the UL inter-cell interference in FDMA SCNs as a lognormal distribution is vital because it allows tractable network performance analysis with closed-form expressions. Compared with the previous works based on empirical studies, our work, for the first time, analytically proved that the conjecture is conditionally correct and the derived condition does not rely on particular shapes/sizes of UE distribution areas. Based on our work, we proposed a new approach to directly and analytically investigate a complex network with *practical deployment of multiple cells* based on the approximation of the UL interference distribution. The proposed approach has the following merits.

1) It can deal with any shape of UE distribution area, which tolerates more practical assumptions, e.g., irregular hotspots, overlapped small cells, etc.
2) It measures the quality of approximation using a closed-form expression and the simulation results validate the tightness of the approximation.
3) It can cope with a large number of small cells by a low computational complexity of analysis.

As future work, we will find a way to relax the derived condition of valid approximation to allow for a wider application of the proposed analysis. Besides, we will consider non-uniform UE distribution and other types of multi-path fading, e.g., Rician fading or Nakagami fading, in our analysis. Also, we will further investigate alternative distributions of the sum of multiple lognormal RVs to make our analysis more accurate.

REFERENCES

[1] D. López Pérez, M. Ding, H. Claussen, and A. H. Jafari, "Towards 1 Gbps/UE in cellular systems: Understanding ultra-dense small cell deployments," *IEEE Commun. Surveys and Tutorials*, Jun. 2015.

[2] J. G. Andrews, F. Baccelli, and R. K. Ganti, "A tractable approach to coverage and rate in cellular networks," *IEEE Transactions on Communications*, vol. 59, no. 11, pp. 3122-3134, Nov. 2011.

[3] T. D. Novlan, H. S. Dhillon and J. G. Andrews, "Analytical modeling of uplink cellular networks," *IEEE Transactions on Wireless Communications*, vol. 12, no. 6, pp. 2669-2679, Jun. 2013.

[4] Y. Zhu, J. Xu, Z. Hu, J. Wang and Y. Yang, "Distribution of uplink inter-cell interference in OFDMA networks with power control," *IEEE International Conf. on Commun.*, Syd., Aus., pp. 5729-5734, Jun. 2014.

[5] S. Singh, N. B. Mehta, A. F. Molisch, and A. Mukhopadhyay, "Moment-matched lognormal modeling of uplink interference with power control and cell selection," *IEEE Transactions on Wireless Communications*, vol. 9, no. 3, pp. 932-938, Mar. 2010.

[6] J. He, Z. Tang, H. Chen, W. Cheng, "Statistical model of OFDMA cellular networks uplink tnterference using lognormal distribution," *IEEE Wireless Commun. Letters*, vol. 2, no. 5, pp. 575-578, Oct. 2013.

[7] M. Ding, D. López Pérez, A. V. Vasilakos, W. Chen, "Dynamic TDD transmissions in homogeneous small cell networks," *IEEE International Conf. on Commun. (ICC)*, Sydney, Australia, pp. 616-621, Jun. 2014.

[8] M. Ding, D. López Pérez, R. Xue, A. V. Vasilakos, W. Chen, "Small cell dynamic TDD transmissions in heterogeneous networks," *IEEE International Conf. on Commun.*, Syd., Aus., pp. 4881-4887, Jun. 2014.

[9] 3GPP, "TS 36.213 (V11.2.0): Physical layer procedures," Feb. 2013.

[10] WiMax Forum, "WiMAX and the IEEE 802.16m Air Interface Standard," Apr. 2010.

[11] M. Ding, D. López Pérez, A. V. Vasilakos, W. Chen, "Analysis on the SINR performance of dynamic TDD in homogeneous small cell networks," *IEEE Global Communications Conference (GLOBECOM)*, Austin, USA, pp. 1552-1558, Dec. 2014.

[12] 3GPP, "TR 36.828 (V11.0.0): Further enhancements to LTE Time Division Duplex (TDD) for Downlink-Uplink (DL-UL) interference management and traffic adaptation," Jun. 2012.

[13] M. Ding, M. Zhang, D. López Pérez, and H. Claussen, "Correlated shadow fading for cellular networks system-level simulations with wrap-around," *IEEE International Conference on Communications (ICC)*, London, UK, pp. 1-7, Jun. 2015.

[14] A. M. D. Turkmani, "Probability of error for M-branch macroscopic selection diversity," *IEE Proceedings on Communications, Speech and Vision*, vol. 139, no. 1, pp. 71-78, Feb. 1992.

[15] I. G. Shevtsova, "An Improvement of Convergence Rate Estimates in the Lyapunov Theorem," *Doklady Mathematics*, vol. 82, no. 3, pp. 862-864, Dec. 2010.

[16] J. Proakis, *Digital Communications (Third Ed.)*, New York: McGraw-Hill, 1995.

[17] N. B. Mehta and A. F. Molisch, "Approximating a sum of random variables with a lognormal," *IEEE Trans. on Wireless Commun.*, vol. 6, no. 7, pp. 2690-2699, Jul. 2007.

[18] M. Abramowitz and I. Stegun, *Handbook of mathematical functions with formulas, graphs, and mathematical tables (Nineth Ed.)*. Dover, 1972.